Time-dependent transport in graphene nanoribbons

Enrico Perfetto,[1] Gianluca Stefanucci,[1,2] and Michele Cini[1,3]
[1]*Dipartimento di Fisica, Universitá di Roma Tor Vergata, Via della Ricerca Scientifica 1, I-00133 Rome, Italy*
[2]*European Theoretical Spectroscopy Facility (ETSF)*
[3]*Consorzio Nazionale Interuniversitario per le Scienze Fisiche della Materia, Unitá Tor Vergata, Via della Ricerca Scientifica 1, 00133 Rome, Italy*

(Received 19 April 2010; revised manuscript received 16 June 2010; published 30 July 2010)

We theoretically investigate the time-dependent ballistic transport in metallic graphene nanoribbons of width W after the sudden switching of a bias voltage. The potential drop is linear across a central part of length L where the current is calculated. During the early transient time the current does not grow linearly in time but remarkably reaches a *temporary plateau*. Such behavior allows us to define a *transient conductivity*, the value of which coincides with the minimal conductivity of two-dimensional graphene. At time L/v_F (v_F being the Fermi velocity) a crossover takes place: the current changes abruptly and saturates at its final steady-state value (second plateau). We show that the two plateaus develop with damped oscillations of totally different nature and demonstrate that the occurrence of the first plateau is independent of the boundary conditions. The transition from quasi-one-dimensional to bulk behavior ($W\to\infty$) is also analyzed.

DOI: 10.1103/PhysRevB.82.035446 PACS number(s): 73.23.Ad, 81.05.U−, 73.63.−b

I. INTRODUCTION

The recent isolation of single layers of carbon atoms[1] has attracted growing attention in the transport properties of graphene-based devices. In these systems unconventional phenomena like the half-integer quantum Hall effect[2] and the Klein tunneling[3] have been observed. Such peculiar behavior stems from the relativistic character of the electrons in the carbon honeycomb lattice; closed to the Dirac point the charge carriers behave as two-dimensional (2D) massless Dirac fermions[4] and have very high mobility.[5] This fact has stimulated intense theoretical and experimental investigations into graphenic ultrafast devices like field effect transistors,[6] *p-n* junction diodes and terahertz detectors.[7] The full control of their electronic response is crucial for optimizing the performance and the study of the real-time dynamics is becoming increasingly important as demonstrated by the recent *time-domain* measurements of the electron motion in a carbon nanotube.[8]

One of the most debated aspects of the transport properties of graphene is the minimum conductivity $\sigma_{\min}$ at the Dirac point. From the theoretical point of view the problem arises from the sensitivity of $\sigma_{\min}$ to the order in which certain limits (zero disorder and zero frequency) are taken,[9] thus producing different values around the quantum e^2/h.[9–12] Very recently Lewkowicz and Rosenstein[13] overcame this ambiguity employing a time-dependent approach and calculated $\sigma_{\min}$ by solving the quench dynamics of 2D Dirac excitations after the sudden switching of a constant electric field.[13,14] Interestingly their approach does not suffer from the use of any regularization related to the Kubo or Landauer formalism and yields $\sigma_{\min}=\pi e^2/2h$.

Time-dependent approaches give access to quantities otherwise difficult to estimate and have the merit to provide a real-time picture of the microscopic dynamics. Despite the large effort in the study of graphenic systems, a genuine real-time analysis of graphene nanoribbons is still missing.

In this paper we calculate the electron dynamics in undoped graphene nanoribbons with *finite width* after the sudden switch-on of an external bias voltage. We study the transition from quasi-one-dimensional (quasi-1D) to bulk and extract $\sigma_{\min}$ as well as the dc conductivity $\sigma_{\rm dc}$ from a one-shot calculation: the time-dependent current does indeed exhibit *two plateaus*. The development of these plateaus occurs with damped oscillations of different nature (frequency and harmonics). Remarkably, this is a universal behavior and is independent of the boundary conditions.

The plan of the paper is the following. In the next section we briefly introduce the tight-binding Hamiltonian describing the nanoribbons and the voltage profile. In the special case of nanoribbons with periodic boundary conditions, we present an equivalent ladder model which is numerically less demanding to treat. Next we focus on the calculation of the time-dependent current flowing across the system after the sudden switching of the bias voltage. The practical implementation method is described in detail. In Sec. III we report the numerical results for nanoribbons of different boundaries (periodic and open) and different chiralites (zigzag and armchair). The summary and main conclusions are drawn in Sec. IV.

II. MODEL AND NUMERICAL METHOD

We consider the system illustrated in Fig. 1. The nanoribbon is divided in three regions: a left (L) and a right (R) semi-infinite graphenic reservoirs and a central (C) region of length $L=aN_c$, with N_c the number of cells along the longitudinal x direction and $a=2.46$ Å, the graphene lattice constant. The width of the ribbon is $W=a\sqrt{3}N_y$, with N_y the number of cells along the transverse y direction. The three regions are linked via transparent interfaces, i.e., the equilibrium system is translationally invariant along x, see Fig. 1.

The system is driven out of equilibrium by the sudden switching of the bias voltage. This is an ultrafast process and excites high energy electrons since the perturbation (steplike in time) contains Fourier components with very large frequencies. It is well known from the Landauer formula that the steady-state current is solely due to the scattering modes lying within the bias window. On the contrary, the short-time

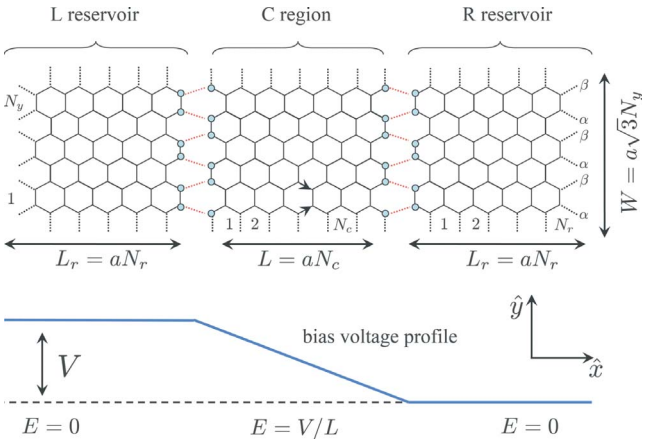

FIG. 1. (Color online) Schematic representation of the system. The nanoribbon has semi-infinite L and R graphenic reservoirs. The linear drop of the bias voltage in region C is also shown.

transient dynamics involves all the electrons within the bandwidth and the frequently used Dirac cone approximation (valid at energies below 1 eV) is not accurate. We therefore use the full tight-binding Hamiltonian

$$H = H_0 + U(t) = v\sum_{\langle i,j\rangle} c_i^\dagger c_j + \theta(t)\sum_i V_i c_i^\dagger c_i, \tag{1}$$

where the spin index has been omitted and $v=2.7$ eV is the hopping integral of graphene. The first sum runs over all pairs of nearest neighbor carbon sites and $c_i^{(\dagger)}$ is the annihilation (creation) operator of a π electron on site i. Here we use the collective index $i=\{p,i_y,i_x\}$ to identify a site in the nanoribbon, such that $p=\alpha,\beta$ indicates the two longitudinal zigzag chains, i_y denotes the cell in the y direction, and i_x is the position in the x direction, see Fig. 1. In Eq. (1) H_0 is the translationally invariant equilibrium Hamiltonian, while $U(t)$ is the bias perturbation with (non-self-consistent) voltage profile[15–17] given by the function V_i

$$V_i = \begin{cases} V/2 & i \in \mathrm{L} \\ V/2 - Ei_x & i \in \mathrm{C} \\ -V/2 & i \in \mathrm{R}, \end{cases} \tag{2}$$

with V the applied voltage and $i_x \in (0,L)$. The electric field $E=V/L$ is uniform and confined in region C. The above modeling of V_i could find a realization in, e.g., a planar junction with the L and R regions on top of metallic electrodes. The time-dependent total current $I(t)$ flowing across the interface in the middle of region C is

$$I(t) = 2\sum_{i_y=1}^{N_y}\sum_{p=\alpha,\beta} I_{i_y}^{(p)}(t), \tag{3}$$

where the factor 2 accounts for spin degeneracy and $I_{i_y}^{(p)}$ is the contribution from the p chain of the i_y-th cell. Our intention is to calculate $I(t)$ at positive times and explore the possibility of defining a meaningful *transient conductivity* before the crossover into the steady-state regime takes place.

We start our analysis by considering the zigzag nanoribbon with periodic boundary conditions (pbc) along y (armchair nanotube).[18–20] Then, the current $I_{i_y}^{(p)}$ is independent of i_y and p, and hence

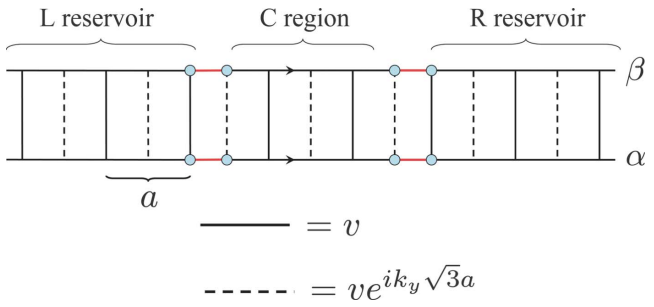

FIG. 2. (Color online) Ladder model for fixed transverse momentum k_y. The bias profile is the same as in Fig. 1.

$$I(t) = 4N_y\bar{I}(t), \tag{4}$$

with $\bar{I}$ the current through a single zigzag chain. Since the transverse momentum $k_y=2\pi n/\sqrt{3}aN_y$ (with $n=0,\ldots N_y-1$) is conserved the current $\bar{I}$ can be written as

$$\bar{I}(t) = \frac{1}{N_y}\sum_{k_y}\bar{I}_{k_y}(t), \tag{5}$$

with $\bar{I}_{k_y}$ the current flowing through the ladder of Fig. 2 with staggered and k_y-dependent transverse hopping. Equation (5) establishes that the total current $I(t)$ can be evaluated by solving N_y independent problems whose dimension is $1/N_y$ times the dimension of the original problem. This provides a huge numerical simplification and how to calculate $\bar{I}_{k_y}(t)$ at fixed k_y is the subject of the rest of this section. We introduce the mixed position-momentum operators

$$c_{\{p,k_y,i_x\}} = N_y^{-1/2}\sum_{i_y} e^{ik_y i_y\sqrt{3}a} c_{\{p,i_y,i_x\}} \tag{6}$$

in terms of which the current $\bar{I}_{k_y}(t)$ can be expressed as

$$\bar{I}_{k_y}(t) = \frac{2ev}{\hbar}\mathrm{Re}[G^<_{\{p,k_y,L/2\};\{p,k_y,L/2+a/2\}}(t,t)], \tag{7}$$

where $G^<$ is the lesser Green's function,

$$G^<_{\{p,k_y,i_x\};\{r,q_y,j_x\}}(t_1,t_2) \equiv i\langle c^\dagger_{\{p,k_y,i_x\}}(t_1)c_{\{r,q_y,j_x\}}(t_2)\rangle, \tag{8}$$

that for $p=r$ is independent of the chain index $p=\alpha,\beta$. The time evolution of $G^<$ is governed by the equation

$$G^<(t_1,t_2)i[e^{iHt_1}f(H_0)e^{-iHt_2}], \tag{9}$$

with f the Fermi distribution function. For each transverse momentum k_y we evaluate $\bar{I}_{k_y}$ by computing the exact time evolution of the ladder in Fig. 2 with reservoirs of *finite length* $L_r=aN_r$. This approach allows us to reproduce the time evolution of the infinite-leads system up to a time $T_{\max}\approx 2L_r/v_F$, where v_F is the Fermi velocity.[21–24] For $t>T_{\max}$ electrons have time to propagate till the far boundary of the leads and back, yielding undesired finite size effects in the calculated current. In all numerical simulations we set $T_{\max}$ much larger than the time to reach the steady-state.

Since the finite-size leads are explicitly included, the approach is alternative to the embedding approach[25–28] (in which the leads are accounted for by an embedding self-energy) and is closer to wave-function based schemes.[29,30] For observable quantities in the central region (like the current that we calculate) there are no corrections up to a time $T_{\max}$ and the results obtained within the present approach and the embedding approach coincide.[23] In the following we will focus on small values of V since we are here interested in linear response properties, although the above propagation scheme can be applied beyond the linear regime.

According to Refs. 23 and 24, the practical calculation of the lesser Green's function $G^<(t,t)$ consists in evaluating the matrix product in Eq. (9) at each time, and this requires the exact numerical diagonalization of the effective ladder Hamiltonian. In the case under consideration this procedure is highly nontrivial due to the peculiar behavior of the electron modes with small k_y (closed to the Dirac point). As we shall see, these are "slow" electrons and the development of $\bar{I}_{k_y}$ to a steady state is numerically very hard to obtain. To overcome such difficulty we use a hybrid basis in which the Hamiltonians of the isolated L and R reservoirs are diagonal while the Hamiltonian of region C remains expressed in the original basis $\{p,k_y,i_x\}$. The diagonal representation of the leads is achieved following the procedure developed by Malysheva and Onipko.[31,32] The enormous advantage of our basis set is clarified below.

For small biases $V \ll \hbar v_F/eW$ the long-time limit of $\bar{I}(t)$ is solely determined by the electrons right at the Dirac point (with $k_y=0$), in agreement with the Landauer formula. However, during the transient *all* transverse modes are excited and contribute to the sum in Eq. (5).[34] The damping time of $\bar{I}_{k_y>0}(t)$ goes like k_y^{-1} and hence the smaller is k_y the longer is the time we need to propagate before the zero-current steady state is approached. To reproduce this feature large values of N_r are needed, thus making the computation in principle too demanding. We, however, observed that after a time of order $\tau_c=L/v_F$ only few low-energy states contribute to $\bar{I}_{k_y}(t)$ for k_y close to the Dirac point. Therefore, for any given $k_y>0$ we introduce an energy cutoff $\Lambda_{k_y} \approx 10\hbar v_F k_y$ and retain only the lead eigenstates of the system in Fig. 2 in the energy window $(-\Lambda_{k_y},\Lambda_{k_y})$. This is possible thanks to the knowledge of the analytic eigenstates of a rectangular graphenic macromolecule.[31,32] Such truncation of the Hilbert space allows us to consider very long leads while treating region C exactly. The time evolution become then feasible and converges with very high accuracy. We would like to recall that the above scheme cannot be applied to nanoribbons with open boundaries. In that case it is not possible to adopt an effective ladder model like the one in Fig. 2 due to the lack of translational invariance along the transverse direction. Thus the computation of the current is much more demanding and only systems with small L and W can be studied, see next the section.

III. RESULTS AND DISCUSSION

In this section we present explicit numerical results obtained for nanoribbons with reservoirs of length $N_r=2000$. In Fig. 3 we show the time-dependent current $I(t)$ calculated for $L \approx 25$ nm ($N_c=100$) and width $W \approx 106$ nm ($N_y=250$) with an applied voltage $V=8\times10^{-4}$ Volt and zero temperature. The ballistic current increases abruptly during the early transient regime, $t \lesssim \hbar/v \equiv \tau_v$. Remarkably, however, for $t>\tau_v$ the current develops a *first plateau* with average current $I_{\min}$ and duration $\tau_c=L/v_F$. Such scenario differs from that in ordinary metals where electrons are uniformly accelerated by the electric field E. Replacing region C with, e.g., a two-dimensional (2D) square lattice model the current would be linear in time up to τ_c, thus producing the well known Drude peak in the current density $j=I/W$ in the bulk limit $L,W \to \infty$. The constant slope γ of the linear behavior $j=\gamma t$ is proportional to the density of states; the latter vanishes in bulk graphene where j does indeed approach a finite value when $t \to \infty$. This subtle compensation is at the origin of the finite minimal dc conductivity $\sigma_{\min}$.[13] In our case electrons initially in the middle of C behave like electrons in a bulk graphene. From Fig. 3 we see that a *finite width* $W \approx 100$ nm is already enough for such compensation to occur. We can, therefore, provide an independent evaluation of $\sigma_{\min}=j/E$: we identify j with $I_{\min}/W$, express E as V/L and obtain

$$\sigma_{\min} = \frac{I_{\min}}{V}\frac{L}{W}. \tag{10}$$

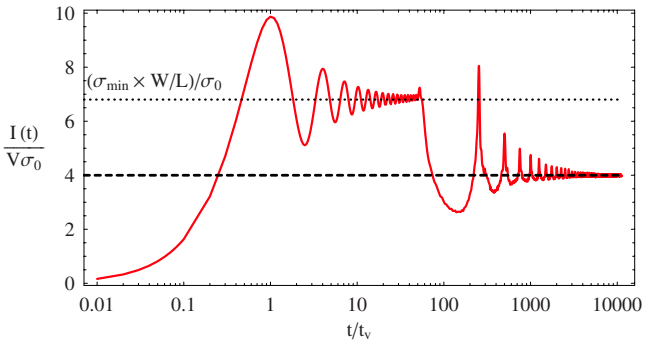

FIG. 3. (Color online) Total current $I(t)$ with geometric parameters $L \approx 25$ nm, $W \approx 106$ nm, $N_r=2000$, and applied voltage $V=8\times10^{-4}$ Volt. Current is in units of $V\sigma_0$, where $\sigma_0=e^2/h$ is the quantum of conductivity and time in units of $t_v=2.5\times10^{-16}$ s. The values of the dc conductivity (dashed line) $\sigma_{\rm dc}/\sigma_0=4$ (Ref. 32) and of the minimal conductivity (dotted line) $(\sigma_{\min}\times W/L)/\sigma_0=\pi/2\times W/L$ are also shown.

Figure 3 shows that our data are consistent with the value $\sigma_{\min}=\pi e^2/2h$ with excellent precision.

The first plateau lasts up to $\tau_c=L/v_F \approx 60t_v$. At times larger than τ_c the electrons start exploring the reservoirs where the electric field is zero. At this point a clear-cut crossover takes place: the current suddenly drops and a standard electron-hole dephasing mechanism sets in. We notice the formation of a *second plateau* whose height corresponds to the value of the final steady-state current $I_{\rm dc}$. As discussed above, however, such value is reached after a very slow damping process during which the current displays decaying oscillations with dominant frequency $\bar{\omega}=2\pi v_F/W$, $\hbar\bar{\omega}$ being the energy spacing between the transverse energy subbands,

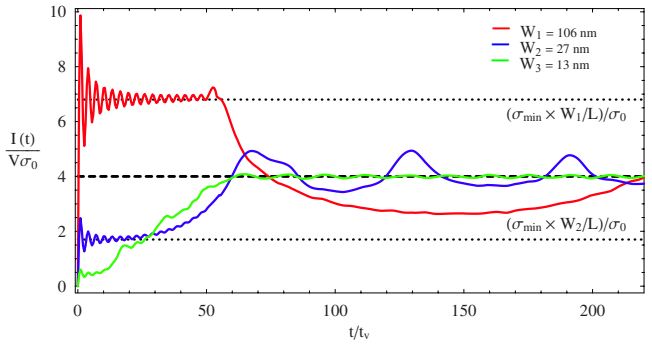

FIG. 4. (Color online) Current $I(t)$ for different widths $W_1=106$ nm, $W_2=27$ nm, $W_3=13$ nm. The rest of parameters are as in Fig. 3.

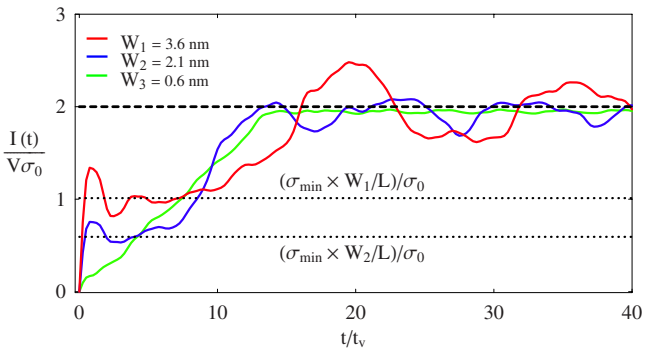

FIG. 5. (Color online) Current $I(t)$ for three different armchair open boundary nanoribbons. The parameters are $L=5.5$ nm, $W_1=3.6$ nm, $W_2=2.1$ nm, $W_3=0.6$ nm and the applied bias is $V=0.03$ Volt. The leads have $N_r=9$ cells. The values of the dc conductivity (dashed line) $\sigma_{dc}/\sigma_0=2$ (Refs. 10 and 32) and of the minimal conductivity (dotted line) $(\sigma_{min}\times W/L)/\sigma_0=\pi/2\times W/L$ are also shown.

see also Fig. 4. We checked numerically that I_{dc} agrees with the Landauer formula and does not depend on L and W provided that $V\ll\hbar v_F/eW$. Thus, the dc conductivity σ_{dc} of the device can simply be extracted from $\sigma_{dc}=I_{dc}/V$. Our data yield $\sigma_{dc}=4e^2/h$ with high numerical accuracy. This value is indeed twice the conductivity of a metallic nanoribbon, as it should when pbc are employed.[32]

Further we investigated the transition from quasi-1D to bulk behavior by varying the width W. In Fig. 4 we see that for narrow ribbons with $W\approx 10$ nm finite-size effects produce a drastic deviation from the ideal graphene bulk. The transient current does not exhibit any plateau but grows with an approximate linear envelope (up to τ_c), in qualitative agreement with the Drude behavior.

We also observe that the plateau at I_{min} develops with damped oscillations of frequency $\omega_0=2v/\hbar$.[13] Interestingly ω_0 is not displayed by any of the individual currents $\bar{I}_{k_y}(t)$, but appears only as a cumulative effect of the sum in Eq. (5). Such frequency is therefore a genuine bulk property and may be related to the resonant effect predicted to occur in optical response of graphene right at $\omega=2v/\hbar$.[33] While the oscillatory behavior during the first plateau is fairly monochromatic and independent of W during the second plateau this is not so. The Fourier decomposition of $I(t)$ reveals a dominant peak at frequency $\bar{\omega}=2\pi v_F/W$ as well as peaks at $\omega_n=n\bar{\omega}$ whose height slowly decreases when $n\to\infty$.

Finally we calculated $I(t)$ also for nanoribbons with open boundaries. As anticipated above, the lack of translational invariance along the transverse direction makes the practical computation of Eq. (9) much more demanding, and only systems with small L and W can be studied within the present approach. In Fig. 5 we show $I(t)$ for three different metallic *armchair* nanoribbons (the honeycomb lattice is rotated of 90 degrees with respect to that of Fig. 1). It can be seen that already for $W\approx 2-4$ nm there is a tendency to form the universal first plateau leading to σ_{min}, while for $W\lesssim 1$ nm the current $I(t)$ grows linearly in time until $t\approx\tau_c$. On the other hand at long times the current tends clearly to the Landauer value, consistent with $\sigma_{dc}=2e^2/h$, independently of the aspect ratio L/W.[10,31] The behavior of $I(t)$ in *zigzag* open-boundaries nanoribbons also displays a first plateau consistent with σ_{min}. However, we observed that the development of the final steady state is substantially longer. Our results demonstrate that boundary effects have no impact on the first universal plateau but only affect the value of the steady-state current.

IV. CONCLUSIONS

In summary we pointed out the subtle difficulties in constructing a reliable method to perform time evolutions of finite width graphene nanoribbons and proposed an efficient numerical scheme to overcome them. We presented a real-time study of the transport properties of these systems in contact with graphenic reservoirs. Since we are mostly interested to the conductance, explicit calculations have been performed within the linear regime, although the approach is not limited to small biases. We showed that for large enough width $W\gtrsim L\gtrsim 20$ nm the time-dependent current displays *two plateaus*. The existence of the first plateau is intimately related to the relativistic spectrum of graphene, and arises from a subtle compensation between vanishing density of states at the Fermi point and diverging current density at long times. From the first plateau we can define a meaningful minimal conductivity and provide an independent evaluation of σ_{min} in bulk graphene. The second plateau is instead related to the dc conductivity σ_{dc}. The formation of the plateaus occurs with damped oscillations of different nature: monochromatic and size independent the first while polychromatic and width dependent the second. We also provide evidence that the two-plateaus behavior is robust against different boundary conditions. To conclude we wish to point out that under ac biases the time-dependent conductivity can be used to extract the optical conductivity σ_{ac} of graphene. It was shown experimentally[35] and explained theoretically[36] that σ_{ac} is almost ω independent and equals σ_{min} with high accuracy over a wide range of frequencies. Remarkably to extract the universal value of σ_{ac} high frequency signals with $\omega\sim 1/t_v$ have been employed.[35] Therefore we believe that a real-time approach like to one presented here is needed to enlighten the crossover from the dc case to ultrafast scenarios in which the period of the ac signal is comparable with the intrinsic hopping time of the bulk system.

[1] K. S. Novoselov, A. K. Geim, S. V. Morozov, D. Jiang, Y. Zhang, S. V. Dubonos, I. V. Gregorieva, and A. A. Firsov, Science **306**, 666 (2004).
[2] K. S. Novoselov, A. K. Geim, S. V. S. V. Morozov, D. Jiang, M. I. Katsnelson, I. V. Gregorieva, S. V. Dubonos, and A. A. Firsov, Nature **438**, 197 (2005); Y. Zhang, Y.-W. Tan, H. L. Stormer, and P. Kim, *ibid.* **438**, 201 (2005).
[3] A. F. Young and P. Kim, Nat. Phys. **5**, 222 (2009); N. Stander, B. Huard, and D. Goldhaber-Gordon, Phys. Rev. Lett. **102**, 026807 (2009).
[4] A. H. Castro Neto, F. Guinea, N. M. R. Peres, K. S. Novoselov, and A. K. Geim, Rev. Mod. Phys. **81**, 109 (2009).
[5] S. V. Morozov, K. S. Novoselov, M. I. Katsnelson, F. Schedin, D. C. Elias, J. A. Jaszczak, and A. K. Geim, Phys. Rev. Lett. **100**, 016602 (2008).
[6] G. Gu, S. Nie, R. M. Feenstra, R. P. Devaty, W. J. Choyke, W. K. Chan, and M. G. Kane, Appl. Phys. Lett. **90**, 253507 (2007).
[7] V. Ryzhii, A. Satou, and T. Otsuji, J. Appl. Phys. **101**, 024509 (2007); F. Xia, T. Mueller, Y.-m. Lin, A. Valdes-Garcia, and P. Avouris, Nat. Nanotechnol. **4**, 839 (2009).
[8] Z. Zhong, Nat. Nanotechnol. **3**, 201 (2008).
[9] K. Ziegler, Phys. Rev. Lett. **97**, 266802 (2006); Phys. Rev. B **75**, 233407 (2007).
[10] N. M. R. Peres, F. Guinea, and A. H. Castro Neto, Phys. Rev. B **73**, 125411 (2006).
[11] J. Tworzydło, B. Trauzettel, M. Titov, A. Rycerz, and C. W. J. Beenakker, Phys. Rev. Lett. **96**, 246802 (2006).
[12] L. A. Falkovsky and A. A. Varlamov, Eur. Phys. J. B **56**, 281 (2007).
[13] M. Lewkowicz and B. Rosenstein, Phys. Rev. Lett. **102**, 106802 (2009).
[14] Y.-X. Wang, L.-P. Shi, and S.-J. Xiong, EPL **87**, 57002 (2009).
[15] A. Pecchia, M. Gheorghe, A. Di Carlo, and P. Lugli, Synth. Met. **138**, 89 (2003).
[16] S. Roche, J. Jiang, L. E. F. Foa Torres, and R. Saito, J. Phys.: Condens. Matter **19**, 183203 (2007).
[17] A. N. Andriotis, M. Menon, and D. Srivastava, J. Chem. Phys. **117**, 2836 (2002).
[18] Y. M. Blanter and I. Martin, Phys. Rev. B **76**, 155433 (2007).
[19] M. I. Katsnelson, Eur. Phys. J. B **51**, 157 (2006).
[20] M. I. Katsnelson and F. Guinea, Phys. Rev. B **78**, 075417 (2008).
[21] N. Bushong, N. Sai, and M. Di Ventra, Nano Lett. **5**, 2569 (2005).
[22] C.-L. Cheng, J. S. Evans, and T. V. Voorhis, Phys. Rev. B **74**, 155112 (2006).
[23] E. Perfetto, G. Stefanucci, and M. Cini, Phys. Rev. B **78**, 155301 (2008).
[24] E. Perfetto, G. Stefanucci, and M. Cini, Phys. Rev. B **80**, 205408 (2009).
[25] A.-P. Jauho, N. S. Wingreen, and Y. Meir, Phys. Rev. B **50**, 5528 (1994).
[26] G. Stefanucci and C.-O. Almbladh, Phys. Rev. B **69**, 195318 (2004).
[27] V. Moldoveanu, V. Gudmundsson, and A. Manolescu, Phys. Rev. B **76**, 085330 (2007).
[28] P. Myöhänen, A. Stan, G. Stefanucci, and R. van Leeuwen, Phys. Rev. B **80**, 115107 (2009); EPL **84**, 67001 (2008).
[29] S. Kurth, G. Stefanucci, C.-O. Almbladh, A. Rubio, and E. K. U. Gross, Phys. Rev. B **72**, 035308 (2005).
[30] P. Bokes, F. Corsetti, and R. W. Godby, Phys. Rev. Lett. **101**, 046402 (2008).
[31] L. Malysheva and A. Onipko, Phys. Rev. Lett. **100**, 186806 (2008).
[32] A. Onipko, Phys. Rev. B **78**, 245412 (2008).
[33] C. Zhang, L. Chen, and Z. S. Ma, Phys. Rev. B **77**, 241402(R) (2008).
[34] We numerically verified when $t \to \infty$ all currents $\bar{I}_{k_y}$ vanish except the one with $k_y = 0$.
[35] R. R. Nair, P. Blake, A. N. Grigorenko, K. S. Novoselov, T. J. Booth, T. Stauber, N. M. R. Peres, and A. K. Geim, Science **320**, 1308 (2008).
[36] T. Stauber, N. M. R. Peres, and A. K. Geim, Phys. Rev. B **78**, 085432 (2008).